Determining the mass transfer coefficient of the water boundary layer at the surface of aquatic integrative passive samplers

Vick Glanzmann [a,*], Kees Booij [b], Naomi Reymond [a], Céline Weyermann [a], Nicolas Estoppey [a]

[a] School of Criminal Justice, University of Lausanne, Batochime building, 1015 Lausanne, Switzerland

[b] PaSOC, Greate Pierwei 25, 8821 LV Kimswerd, The Netherlands

* Corresponding author: Tel.: +41 21 692 46 54; Fax: +41 21 692 46 05; E-mail address: vick.glanzmann@unil.ch

Abstract

Passive sampling devices (PSDs) offer key benefits for monitoring of chemical water quality, but the uptake process of PSDs for hydrophilic compounds still needs to be better understood. Determining mass transfer coefficients of the water boundary layer (k_w) during calibration experiments and in-situ monitoring would contribute towards achieving this; it allows for combining calibration data obtained in different temperature and hydrodynamic conditions and facilitate the translation of laboratory-derived calibration data to field exposure. This study compared two k_w measurement methods applied to extraction disk housings (Chemcatcher), namely alabaster dissolution and dissipation of performance reference compounds (PRCs) from silicone. Alabaster- and PRC-based k_w were measured at four flow velocities (5-40 cm s^{-1}) and two temperatures (11 and 20 °C) in a channel system. Data were compared using a relationship based on Sherwood, Reynolds and Schmidt numbers. Good agreement was observed between data obtained at both temperatures, and for the two methods. Data were well explained by a model for mass transfer to flat plate under laminar flow. It was slightly adapted to provide a semi-empirical model accounting for the effects of housing design on hydrodynamics. The use of PRC-spiked silicone to obtain in-situ integrative k_w for Chemcatcher-type PSDs is also discussed.

Keywords

hydrodynamics, temperature, Chemcatcher, alabaster, performance reference compounds, water quality monitoring, organic contaminants, passive sampling

TOC art

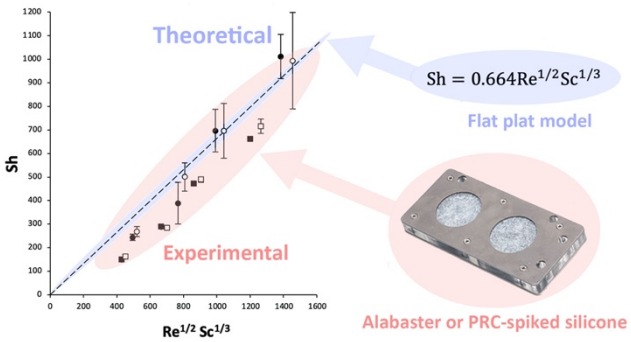

Synopsis

This study shows a good agreement between methods to characterize the hydrodynamics at the surface of Chemcatcher passive samplers.

Introduction

Global surface water is increasingly threatened by emerging organic pollutants (e.g. pesticides or pharmaceuticals) that can have adverse effects on organisms at very low levels [1-4]. Monitoring data is essential for decision-makers to identify the most vulnerable water bodies, prioritize their surveillance, take actions against pollution sources and evaluate the effectiveness of those actions [5, 6]. However, current monitoring programs mainly rely on the analysis of grab water samples and often suffer from lack of temporal representativeness, sensitivity and comparability [5, 7, 8].

Passive sampling – which is based on in-situ accumulation of analytes in a receiving phase – is an alternative to traditional sampling methods that offers key benefits for large-scale monitoring of chemical water quality. First, temporal representativeness is improved because passive sampling devices (PSD) operating in the kinetic sampling stage provide time-weighted average concentrations [9]. Second, passive sampling allows reaching very low limits of quantification thanks to sampling rates (R_S) of several hundreds of millilitres per day (hydrophilic compounds) to several litres per day (hydrophobic compounds) [10, 11]. Third, better comparability of data is achieved because PSDs can be deployed at a large scale, enabling the sorption of pollutants in the same sampling medium at all sampling sites [12].

A wide variety of PSD has been developed. For hydrophobic compounds (log K_{OW} > 3), single-phase low-density polyethylene (LDPE) and silicone rubber (SR) strips have both become popular samplers [13, 14]. The two most used samplers for hydrophilic compounds (log K_{OW} < 3) are the polar organic chemical integrative sampler (POCIS) - i.e. a particulate sorbent material sandwiched between two diffusion limiting membranes - and the polar version of the Chemcatcher® – i.e. a solid-phase extraction disk usually covered by a diffusion limiting membrane [11, 14-16].

Sampling rate (R_S) of time-integrative PSDs needs to be known to infer time-weighted average concentrations from the amount of analyte accumulated in the samplers. R_S of a specific compound depends on (i) PSD properties as well as on (ii) environmental factors (such as hydrodynamics, pH and temperature). Impacts due to PSD materials can be distinguished from impacts due to hydrodynamics [17]:

$$\frac{1}{R_S} = \frac{1}{R_{S,max}} + \frac{1}{Ak_w} \quad (1)$$

where $R_{S,max}$ is the limiting R_S at an infinite flow rate and k_w is the mass transfer coefficient of the water boundary layer (WBL). The uptake of PSDs for hydrophobic compounds is usually controlled by the WBL [13], with a few exceptions when diffusion in polymer is slow [18]. Partial or complete WBL-controlled kinetics may also occur for samplers of hydrophilic compounds [19-22].

The k_w increases with temperature and flow velocity [23, 24]. Determining k_w during calibration and field studies provides a basis for comparing calibration data obtained in different exposure conditions [25], offering the possibility to better understand how R_S depends on water velocities and/or temperature [26]. It can then help choosing the most accurate R_S for specific in-situ conditions. In addition, knowing the contribution of the WBL resistance ($1/k_w$) to the overall mass transfer resistance (A/R_S) facilitates the development of models describing the resistance in PSD materials ($1/R_{S,max}$); this is particularly important to improve the mechanistic understanding of the uptake of PSD for hydrophilic compounds [19, 22].

Alabaster dissolution is a quick and reliable method to measure k_w, and therefore perfectly suitable for calibration studies in laboratory [25]. It is however not adapted to field exposure because the whole alabaster dissipates after a few days. Dissipation of performance and reference compounds (PRCs) provides integrative k_w values over long periods of time. PRCs cannot be used directly with PSDs for hydrophilic compounds as uptake and release of chemicals are anisotropic in this case [26-29]. However, PRC-based k_w can be obtained from silicone PSDs deployed simultaneously to Chemcatcher-type PSDs, in a same housing (example of sampler holder given in Supporting Information Figure S1.1) [13, 30, 31]. When using PCBs as PRCs, kinetics are WBL-controlled because Biot numbers (ratio of internal/external transfer resistance) of PCB transport in silicone are typically smaller than 0.0001 [22].

The k_w is rarely measured during calibration experiments despite its relevance for identifying flow effects on R_S. Instead an equation for mass transfer to a flat plate under laminar flow was used in several studies [22, 26, 32]:

$$k_w = 0.664 \frac{D_w}{L} \left(\frac{UL}{\nu}\right)^{1/2} \left(\frac{\nu}{D_w}\right)^{1/3} \quad (2)$$

where D_w is the diffusion coefficient in water ($m^2\ s^{-1}$), ν is the kinematic viscosity of water ($m^2\ s^{-1}$), U is the water velocity ($m\ s^{-1}$) and L is the length of the flow line along the sorbent-covered part of the

membrane (m). Equation 2 can be expressed as a relationship between Sherwood number ($Sh = k_w L/D_w$), Reynolds number ($Re = UL/\nu$) and Schmidt number ($Sc = \nu/D_w$):

$$Sh = 0.664 Re^{1/2} Sc^{1/3} \quad (3)$$

The goal of this study was to compare two methods – one based on alabaster dissolution and the other on PRC dissipation from silicone – to determine k_w in the case of extraction disk housings (Chemcatcher). Then, this study aimed at testing equation 3 and adapting it to describe as good as possible the experimental data. Finally, the feasibility of the PRC dissipation method to determine in-situ integrative k_w for Chemcatcher will be more particularly discussed.

Materials and Methods

Materials

Analytical grade hexane, ethyl acetate and methanol were obtained from Sigma-Aldrich (Switzerland). Standard solutions of PRCs (biphenyl-d10, PCBs 1, 2, 3, 10, 14, 21, 30, 50, 55, 78, 104, 145 and 204) were purchased from Dr Ehrenstorfer (Germany). ^{13}C-labeled PCBs (^{13}C-PCBs 1, 8, 28, 52, 101, 118, 138, 153, 180) from Cambridge Isotope Laboratories (UK) were used as internal standards. The alabaster disks were purchased from PaSOC (Netherlands). They were shaped into 42 mm diameter and 10 mm thick disks and fitted into a protective PVC housing (one side exposed) with an outer diameter of 51.8 mm. SSP-M823 silicone sheets with a thickness of 0.25 mm were purchased from Shielding Solutions Limited (UK).

Experimental setup

Channel system

Experiments were conducted in a 4-channel system running with lake water (pumped 70 m below the surface of Lake Geneva) inspired by Vermeirssen et al. [21] (see Figure S1.2). The system was made up of a Plexiglass dispenser box (0.70 x 0.40 x 0.45 m), Plexiglass channels (2.00 m long, 0.09 m wide and 0.14 m high) and a plastic receiver tank (0.85 x 0.60 x 0.80 m). The dispenser box delivered the water to the channels through four steel vents (5 cm diameter) fitted with PVC screw caps drilled with holes

of different diameters. Volumetric flowrates delivered to a channel were adjusted by varying the diameter of the hole. The water level was adjusted by changing the size of the opening at the end of each channel (plexiglass gates).

After arriving in the receiver box, water was re-circulated to the dispenser box with an external block pump (NM4 50/16, Brunner AG, Switzerland). The water in the system was continuously refreshed with lake water (dispensed in the receiver box) at a rate of approximately 0.4 L min^{-1}, leading to a renewing of all the water in the system (450 L) within 1 day. Total volume in the system remained constant thanks to an overflow installed on the receiver box.

Exposure conditions

To have a constant water velocity in the channels, the dispenser box was designed with an overflow. Thus, the water level in the box (0.36 m) and the volumetric flow through the vents remained constant. The water velocity in the 4 channels was set at 5, 12, 20 and 40 cm s^{-1} by adjusting the volumetric flow rate (PVC caps) and the water level (gates) in the channels. The flow rates were measured at the beginning of the experiments with a magnetic-inductive flow meter (MF Pro, OTT HydroMet, Germany).

To maintain a constant water temperature, a copper coil (15 m, 18 mm diameter) was installed in the receiver box and connected to a cold water supply (7 °C). A solenoid valve controlled by a temperature regulation system (FOX-1004, Conrad, Switzerland) allowed cold water to run through the copper tube when the temperature exceeded the set value. A logger was used to monitor the temperature during the experiments (Multiline Multi 3620 IDS, WTW, USA).

Before starting the experiments, the system was run for some time allowing the pH to stabilize at 8.1±0.1. The system was placed in a dark environment.

Deployment of alabaster plates and silicone disks

Four main experiments have been conducted: alabaster-based k_w measurements at 11 °C (exp. 1) and 20 °C (exp. 2), and PRC-based k_w measurements at 11 °C (exp. 3) and 20 °C (exp. 4).

Alabaster plates and PRC-spiked silicone disks were mounted in housings that had one side closed and two 40 mm holes on the other side. They were sandwiched between two stainless steel plates (150 x 70

x 2 mm) assembled with 6 screws (drawings in SI, Figure S1.3). Alabaster plates had a thickness of 10 mm; therefore, a plastic block of equivalent thickness was used to hold them in place between the two stainless steel plates (Figure S1.4). Although silicone disks (0.25 mm thick) could be maintained using only the two stainless steel plates, the plastic block was also used in experiments 3 and 4 to keep the same total thickness (Figure S1.5).

The housings were suspended in the channels at mid-height, parallel to the flow, with the surface of the disks situated at 35 mm from the wall of the channel. The length of a channel (2 m) allowed deploying 6 housings (one behind the other) leading to a maximum of 12 disks per channel. These 12 positions were located from 0.85 m to 1.75 m from the beginning of the channel (Figure 1).

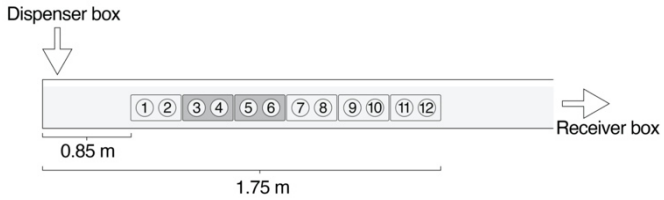

Figure 1: Arrangement of the six housings installed in each channel in experiment 1, leading to 12 usable positions for k_w measurements. In experiments 2, 3 and 4, only positions 3 to 6 were used for k_w determination; plastic disks (dummies) were installed in positions 1 and 2 (to keep the same hydrodynamical conditions) and the three last housings (positions 7 to 12) were not installed.

k_w measurements and calculations

Physicochemical properties

Dynamic viscosity of water (η) was taken from Kestin et al. [33], and water density (ρ) from Jones and Harris [34], which allowed to calculate kinematic viscosity ($\nu = \eta / \rho$).

$D_{w,CaSO4}$ ($m^2\ s^{-1}$) at experimental temperature (11 °C and 20 °C) were obtained from Li and Gregory [35].

$$logD_{w,CaSO4} = -5.407 - \frac{1082}{T} \quad (4)$$

where T is the temperature in Kelvin.

$D_{w,org}$ at 25 °C was calculated from McGowan molar volume (V_{McG} in $cm^3\ mol^{-1}$) as suggested by Schwarzenbach et al. [36];

$$D_{w,org,25°C} = \frac{1.52 \cdot 10^{-8}}{V_{McG}^{0.64}} \quad (5)$$

where $D_{w,org,25°C}$ is given in $m^2\ s^{-1}$. V_{McG} was used rather than molecular weight as it shows better correlation with D_w. Then, $D_{w,org}$ at experimental temperature was determined from $D_{w,org,25°C}$ applying the temperature effect as predicted by Hayduk and Laudie [37].

$$D_{w,org,exp} = D_{w,org,25°C} \left(\frac{\eta_{t=25°C}}{\eta_{t=exp}}\right)^{1.14} \quad (6)$$

where $\eta_{t=25°C}$ and $\eta_{t=exp}$ are dynamic viscosity at 25 °C and experimental temperature, respectively.

Re, Sc, and Sh were calculated from η, ρ, U, D_w, and the characteristic length (L) of the exchange surface. The latter was taken to be equal to the area/diameter ratio (see SI, section S2).

Alabaster-based k_w (experiments 1 and 2)

Alabaster mass loss (Δm) in experiments 1 and 2 was determined by weighing (XS104, Mettler Toledo, Switzerland) the alabaster disks before and after exposure. Mass measurements were preceded by drying plates at 40 °C for 10 min and cooling at room temperature (30 min). To reduce measurement uncertainty, mass losses of approximatively 200 mg were aimed for, by varying the exposure times depending on the velocity (5 hours at 5 cm s^{-1}, 3 hours at 12 cm s^{-1}, 2 hours at 20 cm s^{-1}, 1 hour at 40 cm s^{-1}).

In experiment 1 (11 °C), we measured k_w with 12 alabaster disks on positions 1 to 12 to verify homogeneity of flow conditions along the channels. In the following experiments (exp. 2 to 4), the disks were only deployed at positions 3, 4, 5 and 6 which were the most appropriate (see reasons in Results and Discussion section). To keep similar hydrodynamical conditions, positions 1 and 2 were occupied by a housing without any alabaster/silicone disk. In experiment 2 (20 °C), alabaster-based k_w were measured one time on positions 3 to 6 in each channel.

Alabaster-based k_w for $CaSO_4$ ($k_{w,CaSO4}$) were measured using the method proposed by Booij et al. [25], in the case of a very large water volume:

$$k_{w,CaSO4} = \frac{\Delta m}{A t C_w^*} \quad (7)$$

where A is the surface area of the plate, t is time, Δm is the mass loss after dissolution of alabaster, and C^*_w is the alabaster solubility in water calculated as described by O'Brien et al. [38] using background concentrations of calcium and sulfate (obtained from the local environmental agency).

PRC-based k_w (experiments 3 and 4)

SSP silicone disks were cut with a round punch with a diameter of 42 mm. Before use, the silicone disks were Soxhlet-extracted with ethyl acetate for 100 h to remove oligomers that may interfere with the chemical analysis. The disks were spiked with PRC according to the procedure described in Smedes and Booij [10]. A total of 150 disks were put in a 1 L glass bottle with 0.3 L of methanol. The solution was spiked with 14 PRCs at an amount of 0.3 µg per disk for biphenyl-d10, PRC 1, 2, 3, 10, 14, 21 and 30; 0.15 µg per disk for PRC 50, 55 and 78; and 0.1 µg per disk for PRC 104, 145 and 204. The bottle was shaken under stepwise addition of Milli-Q water over 14 days, ending in 50% (v/v) methanol. Disks were stored at –20 °C in an amber bottle until deployment in the channel system. After 14 days of exposure, they were removed from the water, dried with lint-free wipes and stored at -20 °C in 10 mL amber glass vials (Infochroma, Switzerland) before extraction.

The silicone disks were solvent-extracted with 8 mL of hexane (24 h on a rotary shaker, 30 rpm). A subsample of 0.7 mL of the solvent fraction was spiked with 0.3 mL of the internal standard solution in clean vials. All samples were stored at -20 °C until analysis. The 14 PRC and 10 internal standards were analysed by gas chromatography-tandem mass spectrometry (GC-MSMS, Agilent 7890A GC coupled to an Agilent 7000 Triple Quadrupole MS/MS). The GC-MSMS was equipped with an Agilent HP-5MS column (20 m × 0.2 mm × 0.33 µm). The injection volume was set to 4 µL and injections were performed in splitless mode at 280 °C. Helium was used as carrier gas at 1.2 ml min^{-1}. The temperature program started at 50 °C (0.5 min), increased to 170 °C (50 °C min^{-1}), and then to 250 °C (5 °C min^{-1}) and finally to 320 °C (25 °C min^{-1}) and was held for 8.3 min. The transfer line and ion source temperatures were set at 290 °C and 280 °C respectively. The mass spectrometer was operated in electron impact at −70 eV in the multiple reaction monitoring (MRM) mode (nitrogen was used as collision gas). For each compound, two MRM specific transitions were used.

PRC-based k_w (surface area normalized sampling rate – R_S/A) were determined using a method adapted from Booij and Smedes [30]. All PRCs are used in fitting their retained fractions (*f*) as a function of their sorbent-water partition coefficients (K_{sw}) and $V_{McG}^{0.43}$ using non-linear least square (NLS) regression:

$$f = \frac{C_{PRC}}{C_0} = \exp\left(-\frac{\beta\, t}{m_s K_{sw} V_{McG}^{0.43}}\right) \quad (8)$$

where C_{PRC} is the PRC concentration at time t, C_0 is the initial concentration and β is a proportionality constant that depends on exposure conditions and which is estimated by NLS. In equation 8, V_{McG} is raised to the power 0.43 because k_w is considered proportional to $D_w^{2/3}$, according to hydrodynamical theory [39] and $D_w \sim V_{McG}^{-0.64}$ (see equation 5).

K_{sw} are usually determined at 20 °C in literature [40, 41]. As experiment 3 was conducted at 11 °C, it was necessary to correct those values using the enthalpies of phase transfer from Jonker et al. (2015) (see SI, section S3).

PRC-based k_w were calculated from eq. 8 by:

$$k_{w,org} = \frac{\beta}{A\, V_{McG}^{0.43}} \quad (9)$$

As k_w is compound specific, all PRC-based k_w were expressed for the same organic compound ($k_{w,org}$). PCB 14 was chosen because it showed intermediate dissipation (f = 0.14 to 0.88, see Tables S5.1 to S5.3). Estimating $k_{w,org}$ from PCB 14 data only would be less accurate, because of the high retained fractions at low flow velocities. In addition, obtaining $k_{w,org}$ using eq. 9 makes optimal use of all PRC data, averaging out potential errors in log K_{sw} values of these compounds.

Results and discussion

All alabaster-based k_w, as well as PRC retained fractions obtained at 11 °C and 20°C are given in supporting information, sections S4 and S5.

239 **Preliminary results: characterization of hydrodynamics along the channels**

240 The alabaster-based k_w obtained at 5, 12, 20 and 40 cm s^{-1} during experiment 1 (11 °C) are shown in
241 Figure 2. Average k_w (n=12 at 5 cm s^{-1}, n=36 at 12, 20 and 40 cm s^{-1}) increased with increasing velocity
242 (ANOVA, p= 0.05 and Tukey, α= 0.05). At each flow rate, a higher k_w was measured on position 1
243 compared to the 11 following positions (t-test, p=0.05), revealing that hydrodynamics were slightly
244 different on the first position (higher turbulences due to entrance effects). In the following experiments,
245 alabaster (exp. 2) and silicone (exp. 3 and 4) disks were only deployed on positions 3 to 6. It allowed
246 working with four replicates presenting low variability while minimizing the number of deployed
247 material. For each channel, the relative standard deviation of alabaster-based k_w measured at positions
248 3 to 6 was < 7 %. Those results show that sampler position may impact field-studies and should be
249 further studied, for example by measuring k_w at different positions of sampler holders commonly used
250 in monitoring campaigns.

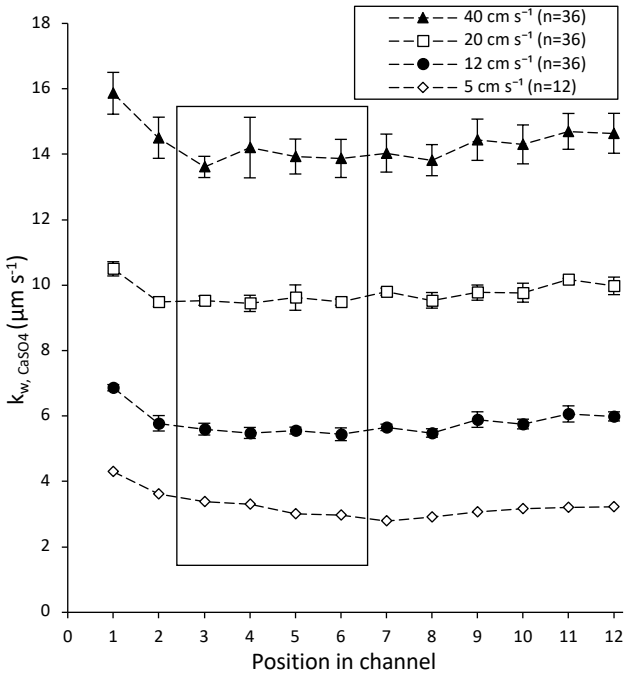

251

252 **Figure 2:** Alabaster-based $k_{w,CaSO4}$ measured on positions 1 to 12 in channels 1 (5 cm s^{-1}), 2 (12 cm s^{-1}), 3 (20 cm s^{-1}) and
253 4 (40 cm s^{-1}). 36 measurements (3 per position) were done in each of the channels 2, 3 and 4; 12 measurements (1 per position)
254 were done in channel 1. Positions 3 to 6 (framed) were conserved for the following experiments (see reasons in the text).

255 **Agreement between alabaster-based k_w, PRC-based k_w and calculated k_w**

256 Values of k_w increased with flow velocity and temperature, and were overall higher for alabaster than
257 for PRCs (Figure 3). These differences are related to WBL thickness (this parameter decreases with

increasing flow velocity), viscosity (η decreases with increasing temperature), and diffusion in water ($D_{w,CaSO4} > D_{w,PCB14}$, and both D_w increase with increasing temperature).

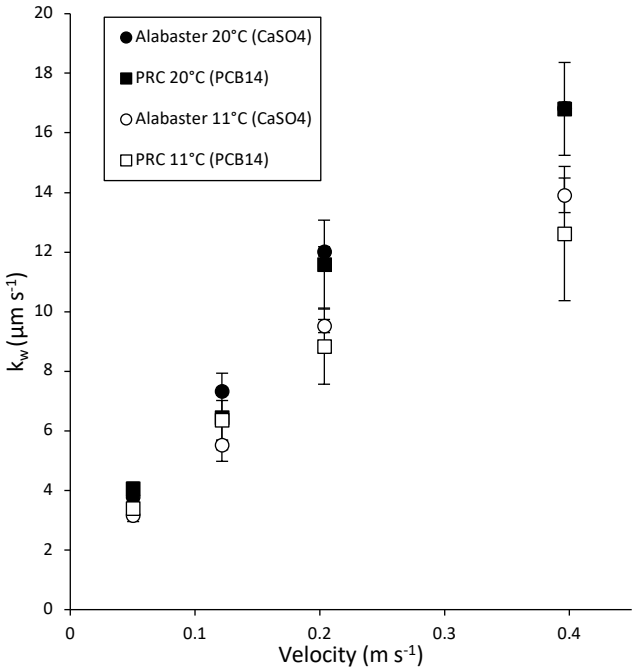

Figure 3: Alabaster-based k_w (circles) and PRC-based k_w (squares) measured at 11 °C (open) and 20 °C (filled) versus velocity.

Estimating $D_{w,CaSO4}$, $D_{w,PCB14}$ and ν at both temperatures (as described in Materials and Methods section) and plotting Sh versus $Re^{1/2}\,Sc^{1/3}$ removed much of the differences caused by temperature (Figure 4). Indeed, the slopes of linear regressions (with origin forcing) obtained at 11 °C and 20 °C were not significantly different (t-test, p=0.05) both with alabaster (0.52±0.06 vs 0.52±0.03) and PRC (0.66±0.08 vs. 0.67±0.08). The slopes of linear regressions obtained by combining PRC data were slightly higher than the ones obtained with alabaster data, but this difference was not statistically different because of the higher scatter of PRC data. Average relative standard deviation of alabaster-based k_w was indeed lower than the one of PRC-based k_w (2.2 % vs. 10.6%), most probably because measurement of mass loss after dissolution of $CaSO_4$ is less prone to errors compared to determination of PRC retained fractions.

The proportionality constant between Sh and $Re^{1/2}\,Sc^{1/3}$ given by equation 3 (0.664) was close to the experimental ones: the lowest slope obtained in this study (0.52, with alabaster) was only 22% smaller than the theoretical value (0.664). Thus, equation 3 gives a surprisingly good description of mass

transfer, considering that present housing and flow conditions differed significantly from the idealized surface (rectangular flat plate with zero thickness) and flow conditions (laminar flow) for which equation 3 is derived. Indeed, the flow in the channels of the present study was turbulent, but Opdyke et al. [42] demonstrated that mass transfer equations for laminar flow also apply for turbulent flow in the short plate limit, i.e. when the diffusive sublayer is well embedded in the viscous sublayer. Further, the steel plate in present housings caused the flow to slow down before it reaches the area where mass transfer occurs, thereby reducing the advection parallel to the surface, and reducing mass transfer. In addition, the presence of the 2 mm rim around the exchange surface may also alter the mass transfer rates. In the case of a flat plate with zero thickness (equation 3), mass transfer already occurs at the edge of the plate, thus explaining why the use of a smaller proportionality constant would even make the description better for Chemcatcher housings. For this purpose, the constant obtained with alabaster data – less scattered than PRC data – was adopted to provide the following semi-empirical model:

$$k_w = \frac{Dw}{\mathrm{L}}\, 0.52 \left(\frac{\nu}{D_w}\right)^{1/3} \left(\frac{UL}{\nu}\right)^{1/2} \qquad (10)$$

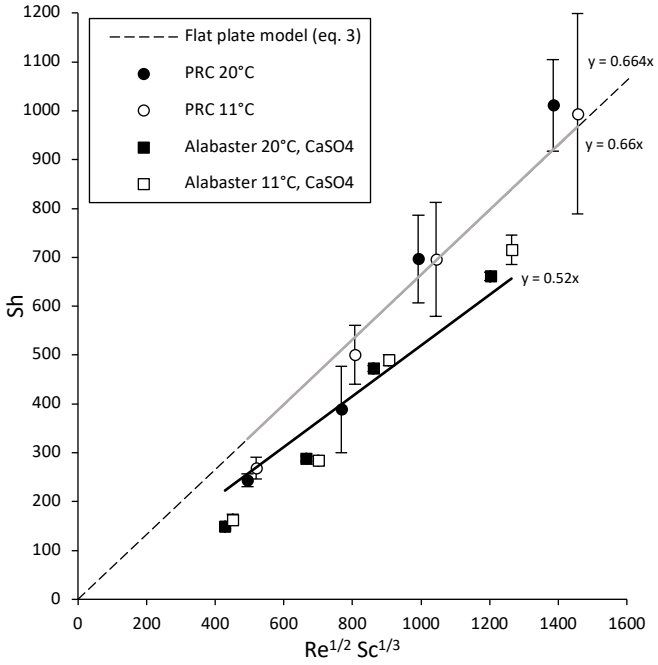

Figure 4: Sherwood number (Sh) for PRC dissipation (circles) and alabaster dissolution (squares) versus $Re^{1/2}Sc^{1/3}$ at 11 °C (open) and 20 °C (filled). Results of linear regression analysis with origin forcing are shown as solid lines (PRC in grey ; alabaster in black). Equation 3 (flat plate model) is shown as a dashed line.

Considerations about the semi-empirical model

Improving the understanding of the uptake of PSD necessitates development and testing (mechanistic) models using calibration data [19, 22]. Many calibration studies however did not measure k_w. Equation 10 provides k_w estimates in the case of extraction disk housings (Chemcatcher). Its use only requires knowing the experimental velocity (U), the diameter of the exposed sorbent/membrane (to determine L) and the experimental temperature (to determine D_w and ν as described in Materials and Methods section). The sampler design needs however to be carefully considered. The model is likely applicable to Chemcatcher designs that are similar to the housing of the present study, e.g. the commercial Chemcatcher 3M Empore (cavity depth of 2.5mm), the Chemcatcher Horizon Atlantic (cavity depth of 4 mm but with an exposed membrane surface that is flush with the outer edge of the housing) [26] or the housings used by Mutzner et al. [20] (cavity depth of 2 mm). Conversely, caution is required when one should want to use the semi-empirical model with initial designs of Chemcatcher that had a cavity depth of 20 mm (e.g. the cylindrical housing proposed by Kingston et al. [43] or the rectangular blocks used by Vermeirssen et al. [27]). Indeed, literature is not unanimous regarding the impact of this change in cavity depth. While Booij and Chen [26] showed that a difference of cavity from 20 mm to 3-7 mm (polycarbonate design) does not largely impact the uptake of atrazine, Lobpreis et al. [44], showed that this same difference can impact the uptake up to a factor of 2. The use of other housings designs (POCIS) and canisters was shown to lead to proportionality coefficients that are much lower (0.41 for POCIS and 0.21 for POCIS inside canisters), revealing that equation 10 would not be appropriate for these situations [45].

To refine the provided semi-empirical model, two aspects should be further studied. First, data obtained at the two lowest velocities (5 and 12 cm s^{-1}) were below the regression lines whereas data obtained at the two highest velocities (20 and 40 cm s^{-1}) were above the regression line (Figure 4). It suggests that the relationships between k_w and U could be slightly different at low and high flows. Such a difference could be due to the rim around the exchange surface. At low flow the surface may be partially shielded from the flow and at increasing flow wake shedding could occur near sharp edges. Second, it cannot be excluded that exponents other than 1/2 and 1/3 apply to the relationship between Sh, Re and Sc, but present data does not allow an assessment of this possibility. When using this specific housing design, we suggest using equation 10 until additional data allow refining the model.

Practical aspects to measure k_w in the field

Measuring accurate in-situ k_w values is essential to correctly translate laboratory-derived calibration data to field exposure. The good agreement between PRC and alabaster data (Figure 4) demonstrate that the use of PRC-spiked silicone deployed in a Chemcatcher is adequate to measure time-integrative k_w over the exposure period. To provide the best possible k_w values, some aspects must however be considered carefully. First, good silicone clamping is essential. In the first experiments, a plastic block was placed between the two stainless steel plates of the housing and a Teflon disk was used to avoid contact between the silicone disk and the plastic block (see reasons in Materials and Methods section). It appeared that the silicone disks were not held completely flat (Figure S1.6). The experiment at 20 °C was repeated by sandwiching the silicone disks between the two stainless steel plates (no Teflon) and by placing the plastic block at the back of the plate without holes (Figure S1.5). The decrease of relative standard deviation between the two experiments (30% vs. 11%) and the better agreement of the proportionality coefficient (0.853 vs. 0.672, Figure S5.4) with the one obtained using alabaster (0.520) indicated that bad clamping can contribute to higher turbulences and more scattered data.

A sufficient portion of PRC-spiked silicone needs to be firmly clamped in the housing to avoid any movement and to hold the disks flat. However, it has to be considered that PRCs from the clamped part first need to diffuse laterally before dissipating. The time scale for lateral diffusion from the rim to the exposed area needs to be much shorter than the time scale of PRC dissipation. Time scale for lateral diffusion is given by the ratio $length^2/D_p$ where the length is the lateral distance and D_p the diffusion coefficient in the polymer. Time scale for PRC dissipation is given by the ratio $K_{pw}m/k_wA$. In the present study, silicone disk and exposed area had a diameter of 42 mm and 40 mm, respectively. Adopting a D_p value of $10^{-10.26}$ m^2 s^{-1} for PCB14 [46], it was determined that the time scale for lateral diffusion (approximately 5 h) was about 70 times shorter than the time scale for PRC dissipation at 40 cm s^{-1} and 20 °C (and about 200 times shorter at 5 cm s^{-1} and 20 °C). A uniform PRC distribution over the whole silicone volume can therefore be assumed.

K_{sw} values of PRCs should be selected based on the best available knowledge because K_{sw} values from different studies may differ up to 0.55 log units, which results in a 3 fold error in k_w [47]. The choice of silicone can thus be guided by the availability of accurate K_{sw} in the literature. In this study, SSP-M823

was used because K_{sw} values for silicone were given by Smedes [40]. The good correspondence between plots of Sh vs. $Re^{1/2}Sc^{1/3}$ for the PRC data at 20°C and 11°C also suggests that the applied temperature correction method for K_{sw} is appropriate. However, as this impact for a 9 °C difference is low (Table S5.5), further studies are needed to confirm the efficiency of the correction for higher differences of temperature.

Implications

During calibration and field experiments, k_w should be measured to provide a comparison basis between studies conducted at different exposure conditions [25]. The results of this study show that both alabaster and PRC dissipation methods can be used to obtain accurate k_w measurements. The alabaster allows to measure k_w over a few hours but it will be completely dissolved after a few days. This method is thus suitable for laboratory experiments under stable conditions. On the other hand, the PRC dissipation method is more appropriate for field measurements where samplers are typically deployed over a few weeks. When none of these methods is – or has been – applied, Equation 10 should be used to estimate k_w based on water velocity and temperature measurements. Equation 10 is valid when using the specific sampler configuration used in this study. It may be extrapolated to similar housing designs (such as commercial Chemcatcher) but this requires further experimental confirmation.

Knowing k_w during calibration studies and field experiments helps choosing the most accurate R_S for specific in-situ conditions and thus provides more accurate TWA water concentrations from concentrations in the samplers.

Supporting Information

Detailed information on channel system and housing; Temperature correction for K_{sw} of PRCs; Additional data from experiments using alabaster dissolution and PRC-spiked silicone. This information is available free of charge via the Internet at http://pubs.acs.org.

Author Information

Corresponding author :

Phone : +41 21 692 46 00; E-mail: vick.glanzmann@unil.ch, celine.weyermann@unil.ch

Notes :

Kees Booij produces and sells alabaster plates for application in passive sampling research.

Acknowledgements

The authors acknowledge Dr. Etiënne L.M. Vermeirssen (Oekotoxzentrum Eawag-EPFL) for his advice in designing the housing and Yves Morier (EPFL) for realizing the drawings and prototypes of the stainless steel plates.

References

1. Fang, W.; Peng, Y.; Muir, D.; Lin, J.; Zhang, X., A critical review of synthetic chemicals in surface waters of the US, the EU and China. *Environment International* **2019,** *131*, 104994; https://doi.org/10.1016/j.envint.2019.104994

2. Schwarzenbach, R.; Egli, T.; T.B., H.; von Gunten, U.; Wehrli, B., Global Water Pollution and Human Health. *Annual Review of Environment and Resources* **2010,** *35*, (1), 109-136; 10.1146/annurev-environ-100809-125342

3. Malaj, E.; von der Ohe, P. C.; Grote, M.; Kühne, R.; Mondy, C. P.; Usseglio-Polatera, P.; Brack, W.; Schäfer, R. B., Organic chemicals jeopardize the health of freshwater ecosystems on the continental scale. *Proceedings of the National Academy of Sciences* **2014,** *111*, (26), 9549-9554; 10.1073/pnas.1321082111

4. Szöcs, E.; Brinke, M.; Karaoglan, B.; Schäfer, R. B., Large Scale Risks from Agricultural Pesticides in Small Streams. *Environmental Science & Technology* **2017,** *51*, (13), 7378-7385; 10.1021/acs.est.7b00933

5. Behmel, S.; Damour, M.; Ludwig, R.; Rodriguez, M. J., Water quality monitoring strategies — A review and future perspectives. *Science of The Total Environment* **2016,** *571*, 1312-1329; https://doi.org/10.1016/j.scitotenv.2016.06.235

6. Hirsch, R. M.; Hamilton, P. A.; T.L., M., U.S. Geological Survey perspective on water-quality monitoring and assessment. *Journal of Environmental Monitoring* **2006,** *8*, 512-518;

7. Xing, Z.; Chow, L.; Rees, H.; Meng, F.; Li, S.; Ernst, B.; Benoy, G.; Zha, T.; Hewitt, L. M., Influences of Sampling Methodologies on Pesticide-Residue Detection in Stream Water. *Archives of Environmental Contamination and Toxicology* **2013,** *64*, (2), 208-218; 10.1007/s00244-012-9833-9

8. Moschet, C.; Vermeirssen, E. L. M.; Seiz, R.; Pfefferli, H.; Hollender, J., Picogram per liter detections of pyrethroids and organophosphates in surface waters using passive sampling. *Water Research* **2014,** *66*, 411-422; https://doi.org/10.1016/j.watres.2014.08.032

9. Vrana, B.; Allan, I. J.; Greenwood, R.; Mills, G. A.; Dominiak, E.; Svensson, K.; Knutsson, J.; Morrison, G., Passive sampling techniques for monitoring pollutants in water. *TrAC Trends in Analytical Chemistry* **2005,** *24*, (10), 845-868;

10. Smedes, F.; Booij, K., Guidelines for passive sampling of hydrophobic contaminants in water using silicone rubber samplers. *ICES Techniques in Marines Envrionmental Sciences* **2012,** *52*; https://dx.doi.org/10.17895/ices.pub.5077

11. Harman, C.; Allan, I. J.; Vermeirssen, E. L. M., Calibration and use of the polar organic chemical integrative sampler—a critical review. *Environmental Toxicology and Chemistry* **2012,** *31*, (12), 2724-2738; 10.1002/etc.2011

12. Lohmann, R.; Muir, D.; Zeng, E. Y.; Bao, L.-J.; Allan, I. J.; Arinaitwe, K.; Booij, K.; Helm, P.; Kaserzon, S.; Mueller, J. F.; Shibata, Y.; Smedes, F.; Tsapakis, M.; Wong, C. S.; You, J., Aquatic Global Passive Sampling (AQUA-GAPS) Revisited: First Steps toward a Network of Networks for Monitoring Organic Contaminants in the Aquatic Environment. *Environ. Sci. Technol.* **2017,** *51*, (3), 1060-1067; 10.1021/acs.est.6b05159

13. Taylor, A. C.; Fones, G. R.; Vrana, B.; Mills, G. A., Applications for Passive Sampling of Hydrophobic Organic Contaminants in Water—A Review. *Critical Reviews in Analytical Chemistry* **2019**, 1-35; 10.1080/10408347.2019.1675043

14. Mills, G. A.; Gravell, A.; Vrana, B.; Harman, C.; Budzinski, H.; Mazzella, N.; Ocelka, T., Measurement of environmental pollutants using passive sampling devices - an updated commentary on the current state of the art. *Environmental Science: Processes & Impacts* **2014,** *16*, (3), 369-373; 10.1039/c3em00585b

15. Vermeirssen, E. L. M.; Dietschweiler, C.; Escher, B. I.; van der Voet, J.; Hollender, J., Uptake and release kinetics of 22 polar organic chemicals in the Chemcatcher passive sampler. *Analytical and Bioanalytical Chemistry* **2013,** *405*, (15), 5225-5236; 10.1007/s00216-013-6878-1

16. Charriau, A.; Lissalde, S.; Poulier, G.; Mazzella, N.; Buzier, R.; Guibaud, G., Overview of the Chemcatcher® for the passive sampling of various pollutants in aquatic environments Part A: Principles, calibration, preparation and analysis of the sampler. *Talanta* **2016,** *148*, 556-571; http://dx.doi.org/10.1016/j.talanta.2015.06.064

17. Fauvelle, V.; Kaserzon, S. L.; Montero, N.; Lissalde, S.; Allan, I. J.; Mills, G.; Mazzella, N.; Mueller, J. F.; Booij, K., Dealing with Flow Effects on the Uptake of Polar Compounds by Passive Samplers. *Environmental Science & Technology* **2017,** *51*, (5), 2536-2537; 10.1021/acs.est.7b00558

18. Narváez Valderrama, J. F.; Baek, K.; Molina, F. J.; Allan, I. J., Implications of observed PBDE diffusion coefficients in low density polyethylene and silicone rubber. *Environmental Science: Processes & Impacts* **2016,** *18*, (1), 87-94; 10.1039/C5EM00507H

19. Endo, S.; Matsuura, Y.; Vermeirssen, E. L. M., Mechanistic Model Describing the Uptake of Chemicals by Aquatic Integrative Samplers: Comparison to Data and Implications for Improved Sampler Configurations. *Environmental Science & Technology* **2019,** *53*, (3), 1482-1489; 10.1021/acs.est.8b06225

20. Mutzner, L.; Vermeirssen, E. L. M.; Mangold, S.; Maurer, M.; Scheidegger, A.; Singer, H.; Booij, K.; Ort, C., Passive samplers to quantify micropollutants in sewer overflows: accumulation behaviour and field validation for short pollution events. *Water Research* **2019,** *160*, 350-360; https://doi.org/10.1016/j.watres.2019.04.012

21. Vermeirssen, E. L. M.; Asmin, J.; Escher, B. I.; Kwon, J.-H.; Steimen, I.; Hollender, J., The role of hydrodynamics, matrix and sampling duration in passive sampling of polar compounds with Empore™ SDB-RPS disks. *Journal of Environmental Monitoring* **2008,** *10*, (1), 119-128; 10.1039/b710790k

22. Booij, K., Passive Sampler Exchange Kinetics in Large and Small Water Volumes Under Mixed Rate Control by Sorbent and Water Boundary Layer. *Environmental Toxicology and Chemistry* **2021,** *40*, (5), 1241-1254; https://doi.org/10.1002/etc.4989

23. Salim, F.; Górecki, T., Theory and modelling approaches to passive sampling. *Environmental Science: Processes & Impacts* **2019,** *21*, (10), 1618-1641; 10.1039/C9EM00215D

24. Booij, K.; Vrana, B.; Huckins, J. N., Theory, modelling and calibration of passive samplers used in water monitoring. In *Passive sampling techniques in environmental monitoring*, Greenwood, R.; Mills, G. A.; Vrana, B., Eds. Elsevier: Amsterdam, 2007; Vol. 48, pp 141-169.

25. Booij, K.; Maarsen, N. L.; Theeuwen, M.; van Bommel, R., A method to account for the effect of hydrodynamics on polar organic compound uptake by passive samplers. *Environmental Toxicology and Chemistry* **2017,** *36*, (6), 1517-1524; 10.1002/etc.3700

26. Booij, K.; Chen, S., Review of atrazine sampling by polar organic chemical integrative samplers and Chemcatcher. *Environmental Toxicology and Chemistry* **2018,** *37*, (7), 1786-1798; 10.1002/etc.4160

27. Vermeirssen, E. L. M.; Dietschweiler, C.; Escher, B. I.; van der Voet, J.; Hollender, J., Transfer Kinetics of Polar Organic Compounds over Polyethersulfone Membranes in the Passive Samplers Pocis and Chemcatcher. *Environmental Science & Technology* **2012,** *46*, (12), 6759-6766; 10.1021/es3007854

28. Shaw, M.; Eaglesham, G.; Mueller, J. F., Uptake and release of polar compounds in SDB-RPS Empore™ disks; implications for their use as passive samplers. *Chemosphere* **2009,** *75*, (1), 1-7; http://dx.doi.org/10.1016/j.chemosphere.2008.11.072

29. Harman, C.; Allan, I. J.; Bäuerlein, P. S., The Challenge of Exposure Correction for Polar Passive Samplers—The PRC and the POCIS. *Environmental Science & Technology* **2011,** *45*, (21), 9120-9121; 10.1021/es2033789

30. Booij, K.; Smedes, F., An Improved Method for Estimating in Situ Sampling Rates of Nonpolar Passive Samplers. *Environmental Science & Technology* **2010,** *44*, (17), 6789-6794; 10.1021/es101321v

31. Uŕik, J.; Vrana, B., An improved design of a passive sampler for polar organic compounds based on diffusion in agarose hydrogel. *Environmental Science and Pollution Research* **2019,** *26*, (15), 15273-15284;

32. Stephens, B. S.; Kapernick, A.; Eaglesham, G.; Mueller, J., Aquatic Passive Sampling of Herbicides on Naked Particle Loaded Membranes: Accelerated Measurement and Empirical Estimation of Kinetic Parameters. *Environmental Science & Technology* **2005,** *39*, (22), 8891-8897; 10.1021/es050463a

33. Kestin, J.; Sokolov, M.; Wakeham, W. A., Viscosity of liquid water in the range −8 °C to 150 °C. *Journal of Physical and Chemical Reference Data* **1978,** *7*, (3), 941-948; 10.1063/1.555581

34. Jones, F. E.; Harris, G. L., ITS-90 Density of Water Formulation for Volumetric Standards Calibration. *J Res Natl Inst Stand Technol* **1992,** *97*, (3), 335-340; 10.6028/jres.097.013

35. Li, Y.-H.; Gregory, S., Diffusion of ions in sea water and in deep-sea sediments. *Geochimica et Cosmochimica Acta* **1974,** *38*, (5), 703-714; https://doi.org/10.1016/0016-7037(74)90145-8

36. Schwarzenbach, R. P.; Gschwend, P. M.; Imboden, D. M., *Environmental Organic Chemistry*. 3rd ed.; John Wiley & Sons: Hoboken, NJ, USA, 2016.

37. Hayduk, W.; Laudie, H., Prediction of diffusion coefficients for nonelectrolytes in dilute aqueous solutions. *AIChE Journal* **1974,** *20*, (3), 611-615; https://doi.org/10.1002/aic.690200329

38. O'Brien, D. S.; Booij, K.; Hawker, D. W.; Mueller, J. F., Method for the in Situ Calibration of a Passive Phosphate Sampler in Estuarine and Marine Waters. *Environmental Science & Technology* **2011,** *45*, (7), 2871-2877; 10.1021/es101645z

39. Rusina, T. P.; Smedes, F.; Koblizkova, M.; Klanova, J., Calibration of silicone rubber passive samplers: Experimental and modeled relations between sampling rate and compound properties. *Environmental Science and Technology* **2010,** *44*, (1), 362-367;

40. Smedes, F., SSP silicone–, lipid– and SPMD–water partition coefficients of seventy hydrophobic organic contaminants and evaluation of the water concentration calculator for SPMD. *Chemosphere* **2019,** *223*, 748-757; https://doi.org/10.1016/j.chemosphere.2019.01.164

41. Smedes, F.; Geertsma, R. W.; Zande, T. v. d.; Booij, K., Polymer−Water Partition Coefficients of Hydrophobic Compounds for Passive Sampling: Application of Cosolvent Models for Validation. *Environmental Science & Technology* **2009,** *43*, (18), 7047-7054; 10.1021/es9009376

42. Opdyke, B. N.; Gust, G.; Ledwell, J. R., Mass transfer from smooth alabaster surfaces in turbulent flows. *Geophysical Research Letters* **1987,** *14*, (11), 1131-1134;

43. Kingston, J. K.; Greenwood, R.; Mills, G. A.; Morrison, G. M.; Bjorklund Persson, L., Development of a novel passive sampling system for the time-averaged measurement of a range of organic pollutants in aquatic environments. *Journal of Environmental Monitoring* **2000,** *2*, (5), 487-495; 10.1039/b003532g

517 44. Lobpreis, T.; Vrana, B.; Dominiak, E.; Dercová, K.; Mills, G. A.; Greenwood, R., Effect of
518 housing geometry on the performance of Chemcatcher passive sampler for the monitoring of
519 hydrophobic organic pollutants in water. *Environ Pollut* **2008,** *153*, (3), 706-10;
520 10.1016/j.envpol.2007.09.011

521 45. Booij, K.; Chen, S.; Trask, J. R., POCIS Calibration for Organic Compound Sampling in Small
522 Headwater Streams. *Environmental Toxicology and Chemistry* **2020,** *39*, (7), 1334-1342;
523 https://doi.org/10.1002/etc.4731

524 46. Rusina, T. P.; Smedes, F.; Klanova, J., Diffusion coefficients of polychlorinated biphenyls and
525 polycyclic aromatic hydrocarbons in polydimethylsiloxane and low-density polyethylene polymers.
526 *Journal of Applied Polymer Science* **2010,** *116*, (3), 1803-1810; 10.1002/app.31704

527 47. Lohmann, R.; Booij, K.; Smedes, F.; Vrana, B., Use of passive sampling devices for monitoring
528 and compliance checking of POP concentrations in water. *Environmental Science and Pollution*
529 *Research* **2012,** *19*, (6), 1885-1895; 10.1007/s11356-012-0748-9

530